J Geod (2008) 82:431–443
DOI 10.1007/s00190-007-0195-4

ORIGINAL ARTICLE

Compactly supported radial covariance functions

G. Moreaux

Received: 21 March 2007 / Accepted: 31 October 2007 / Published online: 23 November 2007

Abstract The Least-squares collocation (LSC) method is commonly used in geodesy, but generally associated with globally supported covariance functions, i.e. with dense covariance matrices. We consider locally supported radial covariance functions, which yield sparse covariance matrices. Having many zero entries in the covariance matrice can both greatly reduce computer storage requirements and the number of floating point operations needed in computation. This paper reviews some of the most well-known compactly supported radial covariance functions (CSRCFs) that can be easily substituted to the usually used covariance functions. Numerical experiments reveals that these finite covariance functions can give good approximations of the Gaussian, second- and third-order Markov models. Then, interpolation of KMS02 free-air gravity anomalies in Azores Islands shows that dense covariance matrices associated with Gaussian model can be replaced by sparse matrices from CSRCFs resulting in memory savings of one-fortieth and with 90% of the solution error less than 0.5 mGal.

Keywords Least-squares · Comactly supported covariance functions · Large linear systems · Sparse matrices

1 Introduction

Least-squares collocation (e.g., Moritz 1989) is a flexible and powerful technique to both interpolate and predict continuous fields, such as the anomalous gravity field of the Earth, from any set of discretly and noisy observations of some linear functionals of that field (gravity anomalies and height anomalies for instance). Moreover, one of the major key success of LSC lies in the fact that it also gives access to the prediction errors. To compute the LSC solution, one has to solve a linear system with as many equations as the number of data where the matrix is the covariance matrix of the observations. Then, since most of geophysical covariance models (e.g., Gaussian model, second- and third-order Markov models) are globally supported, its covariance matrices are generally dense in terms of not having any zero entries, thus posing severe numerical problems in solution feasibility.

To overcome that practical problem of LSC, various methods have been proposed to reduce the computational burden by introducing some zeros in the matrix of the linear system. The objective is to get a sparse matrix, which gives crucial advantages when dealing with massive datasets. Firstly, sparse matrices give great savings in storage and computation memory by not storing many zero entries. For example, the storage requirement for an $n \times n$ full matrix is $8n^2$ bytes, if we use 8-bytes for real numbers and 4-bytes for integers. A sparse matrix is stored as a list of its nonzero elements together with the row index and column pointer in the so-called compressed sparse row format (e.g., Saad 1996). Therefore, the storage requirement of an $n \times n$ sparse matrix with nz nonzero entries is $12nz + 4n$ bytes, which can be much less than $8n^2$ if nz/n^2 is small.

Secondly, sparse matrix algorithms require much less computation time than standard algorithms by avoiding arithmetic operations on zero elements (e.g., Saad 1996). For example, the complexity of solving a linear system is $\mathcal{O}(n^3)$ for a full $n \times n$ matrix and is approximately $\mathcal{O}(n)$ for a sparse matrix with certain structures.

Thus, if it is possible to use a covariance function with a finite support, i.e. a covariance function that is identically zero outside of a fixed distance, then the covariance matrix

This article is dedicated to Cerbère.

G. Moreaux (✉)
La Roque de Scieurac, 32100 Condom, France
e-mail: g.moreaux@free.fr

becomes sparse. This quest is supported by the fact that in many statistical models correlations are negligible beyond a certain distance when compared with the variance. Then, the the choice of the compactly supported function becomes the key point of the method. The first idea could be to truncate the covariance function beyond a cut-off distance that is to neglect small coefficients of the covariance matrix. Even if that option can give satisfactory numerical results (Rygaard et al. 1997; Tóth and Völgyesi 2007), this naive thresholding very often destroys positive-definiteness of the truncated matrix so the solution of the sparse linear system may not exist. Therefore, we should require that the compactly supported function be also positive definite. This requirement can be fulfilled by either tapering (Furrer et al. 2005) the globally supported covariance function C, i.e. by multiplying C with a locally supported covariance function C_d, or to approximate C by a locally supported covariance function $\widetilde{C}$ (Sansò and Schuh 1987).

An objection to tapering is that it may not be effective even for a spatial covariance with short range correlations since C and $C \times C_d$ would be very different. Thus, in line with previous studies and experiments with compactly supported spherical covariance functions (e.g., Arabelos and Tscherning 1996; Schreiner 1997; Moreaux et al. 1999), in the present contribution I will introduce compactly supported radial covariance functions (CSRCFs) with closed-form expressions. By radial functions, I mean functions of the Cartesian distance by opposition to the spherical distance. Such radial functions are commonly used in geodesy in case of flat earth, i.e. in planar approximations. These CSRCFs were introduced by Schaback and Wendland (1993) and later expanded by Wu (1995). Further developments were provided by Wendland (1995) and Gneiting (1999). Then, Floater and Iske (1996) first adopted CSRBFs for multistep scattered data interpolation. These CSRCFs have also been successfully used in frameworks like environmental modelling (Wong et al. 1999), implicit surface registration (Morse et al. 2001), medical images visualization (Fornefett et al. 1999; Wachowiak et al. 2004) and economy (Hon and Zhou, 2000).

This contribution is organized as follows. I start in Sect. 2 by an overview about the most well-known CSRCFs in $\mathbb{R}^3$. In Sect. 3, I first show how to approximate Gaussian, second-order and third-order Markov models by the finite covariance functions previously introduced. Then, interpolations of KMS02 (Andersen et al. 2004) free-air gravity anomalies in the area of Azores Islands demonstrate that full systems arising from the modelization of the emprical covariance function by the Gaussian model can be satisfactorily, in terms of memory saving and of differences between the "full" and "finite" predictions, replaced by a sparse system deduced from the use of CSRCFs. Finally, conclusions and perspectives of this work are presented in Sect. 4.

2 Compactly supported radial covariance functions

In the sequel, I denote by Φ_3 the class of all continuous functions $\varphi : [0, \infty) \to \mathbb{R}$ such that $\varphi(0) = 1$ and the radially symmetric function $\varphi(\|.\|_2)$ is positive-definite on $\mathbb{R}^3$. Note that functions of Φ_3 are isotropic and yield covariance functions in planar approximations.

Hereafter, L is the correlation-length of the covariance function φ, i.e. the distance for which the function has decreased to half of its value at $r = 0$:

$$\varphi(L) = \frac{1}{2}\,\varphi(0). \tag{1}$$

Moreover, in this contribution, ξ designates the so-called curvature parameter as defined by Moritz (1989). For functions with first radial derivatives which vanish at origin, the curvature parameter is expressed by

$$\xi = -\frac{L_{\text{cor}}^2}{\varphi(0)}\,\frac{\partial^2\varphi}{\partial r^2}(0). \tag{2}$$

2.1 CSRCFs from Wendland

The starting point of Wendland's (1995) work is the truncated power function $\varphi_l(r) = (1-r)_+^l$, which is a member of Φ_3 if, and only if, $l \geq 2$ (Askey, 1973). Since the truncated power function is not smooth at zero, according to Kasper (1971) who argued that covariance function shoud approach zero at zero distance as gravity anomalies depend on the mass distribution of the earth, which tends to be locally constant, Wendland defined

$$\varphi_{l,k}^{\text{We}}(r) = c_{l,k}\, I^k \varphi_l(r), \quad r \geq 0, \quad k = 0, 1, \ldots, \tag{3}$$

where the constant $c_{l,k}$ is such that $\varphi_{l,k}^{\text{We}}(0) = 1$, and where

$$I\varphi(r) = \int_r^\infty t\,\varphi(t)\,\mathrm{d}t, \quad r \geq 0, \tag{4}$$

$$I^k\varphi = I\left(I^{k-1}\varphi\right), \quad k \geq 1. \tag{5}$$

Then, $\varphi_{l,k}^{\text{We}}$ is a member of Φ_3 if, and only if, $l \geq k+2$. Moreover, there exists a real polynomial $p_{l,k}$ of degree k such that

$$\varphi_{l,k}^{\text{We}}(r) = (1-r)_+^{l+k}\; p_{l,k}(r), \tag{6}$$

so $\varphi_{l,k}^{\text{We}}$ is smooth, $2k$ differentiable at zero, possesses $k+l-1$ continuous derivatives around one and has compact support [0; 1]. From Eqs. (3) and (4), we can deduce that Wendland's functions satisfy the following properties:

$$\frac{\partial\varphi_{l,k}^{\text{We}}}{\partial r}(0) = 0, \quad \frac{\partial\varphi_{l,k}^{\text{We}}}{\partial r}(1) = 0, \quad \forall l \geq 1, \quad \forall k \geq 1, \tag{7}$$

$$\varphi_{l,k}^{\text{We}} \geq 0, \quad \forall l \geq 0, \quad \forall k \geq 0. \tag{8}$$

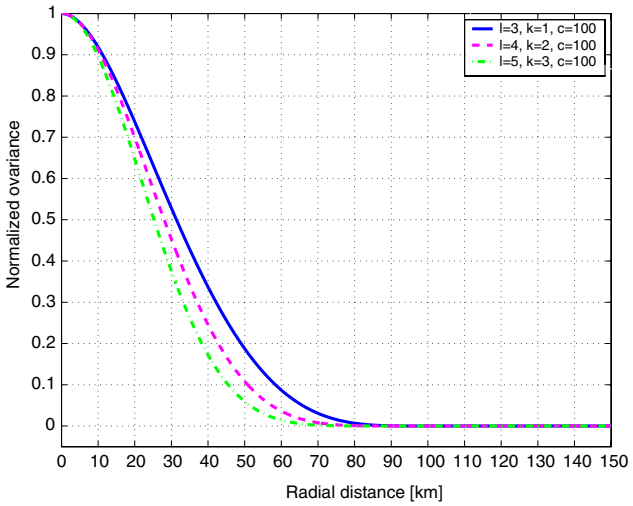

Fig. 1 Examples of Wendland's CSRCFs

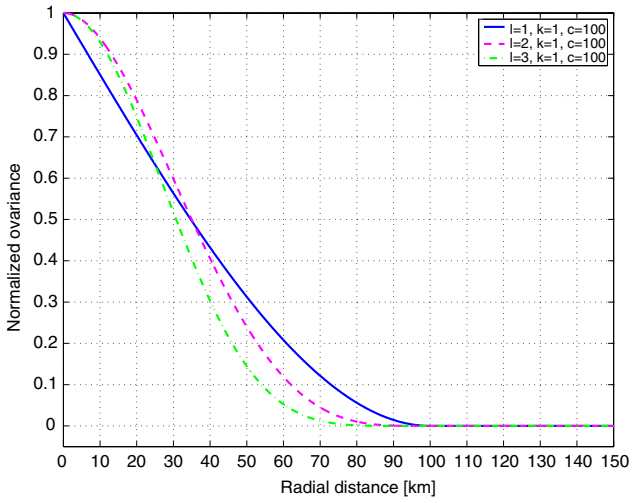

Fig. 2 Examples of Wu's CSRCFs

Below, I list $\varphi^{\mathrm{We}}_{l,k}(\cdot, c) \equiv \varphi^{\mathrm{We}}_{l,k}(./c)$ functions of Φ_3 for $k = 1, 2, 3$; for examples, functions corresponding to $l = k + 2$ with $c = 100$ km are depicted in Fig. 1.

$$\varphi^{\mathrm{We}}_{3,1}(r, c) = \left(1 - \frac{r}{c}\right)^4_+ \left(1 + 4\frac{r}{c}\right), \tag{9}$$

$$\varphi^{\mathrm{We}}_{4,1}(r, c) = \left(1 - \frac{r}{c}\right)^5_+ \left(1 + 5\frac{r}{c}\right), \tag{10}$$

$$\varphi^{\mathrm{We}}_{4,2}(r, c) = \left(1 - \frac{r}{c}\right)^6_+ \left[1 + 6\frac{r}{c} + \frac{35}{3}\left(\frac{r}{c}\right)^2\right], \tag{11}$$

$$\varphi^{\mathrm{We}}_{5,2}(r, c) = \left(1 - \frac{r}{c}\right)^7_+ \left[1 + 7\frac{r}{c} + 16\left(\frac{r}{c}\right)^2\right], \tag{12}$$

$$\varphi^{\mathrm{We}}_{5,3}(r, c) = \left(1 - \frac{r}{c}\right)^8_+ \left[1 + 8\frac{r}{c} + 25\left(\frac{r}{c}\right)^2 + 32\left(\frac{r}{c}\right)^3\right]. \tag{13}$$

From Eqs. (6) and (7), the curvature parameter $\xi^{\mathrm{We}}_{l,k}$ of the Wendland's function $\varphi^{\mathrm{We}}_{l,k}$ is given by

$$\xi^{\mathrm{We}}_{l,k} = -\left(\frac{L^{\mathrm{We}}_{l,k}}{c}\right)^2 \left[(l + k - 1)(l + k)\, p_{l,k}(0) - 2(l + k)\, p'_{l,k}(0) + p''_{l,k}(0)\right]. \tag{14}$$

Furthermore, since the real polynomial $p_{l,k}$ of degree k satisfy

$$p_{l,k}(0) = 1, \quad p'_{l,k}(0) = l + k, \tag{15}$$

the curvature parameter expression simplifies to

$$\xi^{\mathrm{We}}_{l,k} = \left(\frac{L^{\mathrm{We}}_{l,k}}{c}\right)^2 \left[(l + k + 1)(l + k) + p''_{l,k}(0)\right], \tag{16}$$

where the correlation length $L^{\mathrm{We}}_{l,k}$ of all the previously listed functions is between $c/4$ and $c/3$. For more details on these functions, we refer to Wendland (1995) and Wendland (1998).

2.2 CSRCFs from Wu

The construction of the CSRCFs due to Wu (1995) starts with

$$f_l(r) = \left(1 - r^2\right)^l_+, \quad l \geq 0, \tag{17}$$

then takes univariate derivatives of convolutions

$$\varphi^{\mathrm{Wu}}_{l,k} = c_{l,k}\, D^k\, (f_l * f_l)\, (r) \equiv c_{l,k}\, D^k \varphi^{\mathrm{Wu}}_{l,0}, \quad 0 \leq k \leq l, \tag{18}$$

for $D = -\frac{1}{r}\frac{\mathrm{d}}{\mathrm{d}r}$ and where the constant $c_{l,k}$ is such that $\varphi^{\mathrm{Wu}}_{l,k}(0) = 1$. It is straightforward to show that $\varphi^{\mathrm{Wu}}_{l,k}$ belongs to Φ_3 for $k \geq 1$ and possesses $2(l-k)$ derivatives. Moreover, there exists a unique real polynomial q_{2l-k} of degree $2l - k$ such that

$$\varphi^{\mathrm{Wu}}_{l,k}(r) = (1 - r)^{2l-k+1}_+ \; q_{2l-k}(r). \tag{19}$$

Based on Eqs. (17) and (18), it is easy to show that:

$$\frac{\partial \varphi^{\mathrm{Wu}}_{l,k}}{\partial r}(0) = 0, \tag{20}$$

$$\frac{\partial \varphi^{\mathrm{Wu}}_{l,k}}{\partial r}(1) = 0, \quad \forall l \geq k + 1, \tag{21}$$

$$\varphi^{\mathrm{Wu}}_{l,k} \geq 0, \quad \forall l \geq 0, \quad \forall k \geq 0, \tag{22}$$

$$\varphi^{\mathrm{Wu}}_{l,k} \in C^{2(l-k)} \text{ around } 0, \quad \varphi^{\mathrm{Wu}}_{l,k} \in C^{2l-k} \text{ around } 1. \tag{23}$$

The following equations give explicit formulae of Wu's (1995) functions $\varphi^{\mathrm{Wu}}_{l,k}(\cdot, c) \equiv \varphi^{\mathrm{Wu}}_{l,k}(\cdot/c)$ $(k = 1, 2)$ which can be visualized for arbitrary values of $k = 1$ and $c = 100$ km in Fig. 2.

$$\varphi^{\mathrm{Wu}}_{1,1}(r,c)=\left(1-\frac{r}{c}\right)^2_+\left(1+\frac{1}{2}\frac{r}{c}\right), \tag{24}$$

$$\varphi^{\mathrm{Wu}}_{2,1}(r,c)=\left(1-\frac{r}{c}\right)^4_+\left[1+4\frac{r}{c}+3\left(\frac{r}{c}\right)^2+\frac{3}{4}\left(\frac{r}{c}\right)^3\right], \tag{25}$$

$$\varphi^{\mathrm{Wu}}_{2,2}(r,c)=\left(1-\frac{r}{c}\right)^3_+\left[1+\frac{9}{8}\frac{r}{c}+\frac{3}{8}\left(\frac{r}{c}\right)^2\right], \tag{26}$$

$$\varphi^{\mathrm{Wu}}_{3,1}(r,c)=\left(1-\frac{r}{c}\right)^6_+\left[1+6\frac{r}{c}+\frac{82}{6}\left(\frac{r}{c}\right)^2+12\left(\frac{r}{c}\right)^3+5\left(\frac{r}{c}\right)^4+\frac{5}{6}\left(\frac{r}{c}\right)^5\right], \tag{27}$$

$$\varphi^{\mathrm{Wu}}_{3,2}(r,c)=\left(1-\frac{r}{c}\right)^5_+\times\left[1+5\frac{r}{c}+6\left(\frac{r}{c}\right)^2+\frac{25}{8}\left(\frac{r}{c}\right)^3+\frac{5}{8}\left(\frac{r}{c}\right)^4\right]. \tag{28}$$

From Eqs. (19) and (20), and as the polynomial q_{2l-k} of degree $2l-k$ satisfies $q_{2l-k}(0)=1$, the curvature parameter of $\varphi^{\mathrm{Wu}}_{l,k}$ is expressed by

$$\xi^{\mathrm{Wu}}_{l,k}=-\left(\frac{L^{\mathrm{Wu}}_{l,k}}{c}\right)^2\left[(2l-k+1)(2l-k)-2(2l-k+1)p'_{2l-k}(0)+p''_{2l-k}(0)\right] \tag{29}$$

where the correlation length $L^{\mathrm{Wu}}_{l,k}$ for $(l,k)\in\{(1,1),\ (2,1)\}$ is between $c/3$ and $c/2$ whereas it is between $c/4$ and $c/3$ for $(l,k)\in\{(2,2),\ (3,1),\ (3,2)\}$.

To conclude on Wu's functions, Wendland (1995) shown that these functions are connected with the so-called Euclid's Hat X^{2l+1} by $\varphi^{\mathrm{Wu}}_{l,k}(r)\doteq I^{l_k}X^{2l+1}(r)$ with theoperator I as defined by Eq. (4) and where $\doteq$ means equality up to a constant.

2.3 CSRCFs from Buhmann

If δ, ρ, λ and α are reals such that

$$0<\delta<0.5,\quad \rho\geq 1,\lambda>0,\quad -1<\alpha\leq\frac{1}{2}(\lambda-1), \tag{30}$$

then, from Buhmann (2000), the radial function

$$\varphi^{\mathrm{Bu}}_{\alpha,\delta,\rho,\lambda}(r)=\int_0^\infty\left(1-\frac{r^2}{\beta}\right)^\lambda_+\left(1-\beta^\delta\right)^\rho_+\beta^\alpha\,\mathrm{d}\beta \tag{31}$$

is a member of Φ_3. Furthermore, $\varphi^{\mathrm{Bu}}_{\alpha,\delta,\rho,\lambda}$ is at least $1+\lfloor 2\alpha\rfloor$ times continuously differentiable. Here, $\lfloor\cdot\rfloor$ denotes the largest integer not exceeding x. Moreover, from Eq. (31), it is easy to show that Buhmann's functions satisfy

$$\frac{\partial\varphi^{\mathrm{Bu}}_{\alpha,\delta,\rho,\lambda}}{\partial r}(0)=0,\quad \frac{\partial\varphi^{\mathrm{Bu}}_{\alpha,\delta,\rho,\lambda}}{\partial r}(1)=0,\quad \varphi^{\mathrm{Bu}}_{\alpha,\delta,\rho,\lambda}\geq 0, \tag{32}$$

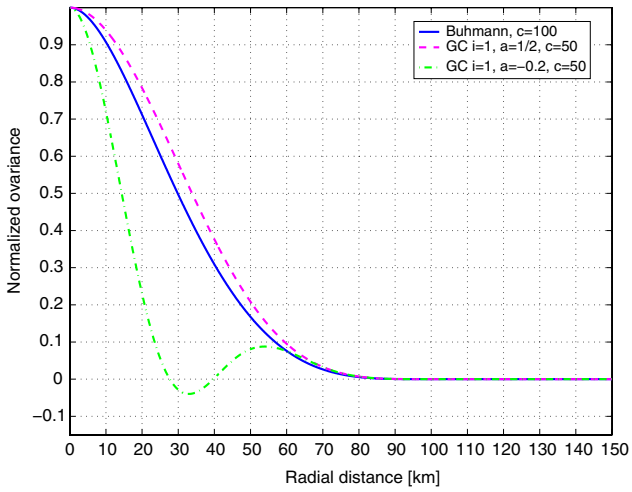

Fig. 3 Examples of Buhmann's and Gaspari and Cohn's CSRCFs

for all α, δ, ρ, λ satisfying (30). For $\alpha=\delta=0.5$, $\rho=1$ and $\lambda=2$, from (31), we get the radial function

$$\varphi^{\mathrm{Bu}}_{1/2,1/2,1,2}(r,c)\equiv\varphi^{\mathrm{Bu}}_{1/2,1/2,1,2}(r/c) \tag{33}$$

$$=\left[12\left(\frac{r}{c}\right)^4\log\left(\frac{r}{c}\right)-21\left(\frac{r}{c}\right)^4+32\left(\frac{r}{c}\right)^3-12\left(\frac{r}{c}\right)^2+1\right]\left(1-\frac{r}{c}\right)_+ \tag{34}$$

which is twice continuously differentiable and illustrated by Fig. 3 for $c=100$ km. Buhmann (2000) shows that both Wendland's and Wu's functions admit a convolution representation of Eq. (31) for suitable α, δ, ρ and λ. Finally, after straighforward computations,

$$\xi^{\mathrm{Bu}}_{1/2,1/2,1,2}=24\left(\frac{L^{\mathrm{Bu}}_{1/2,1/2,1,2}}{c}\right)^2 \tag{35}$$

with $\frac{c}{4}\leq L^{\mathrm{Bu}}_{1/2,1/2,1,2}\leq\frac{c}{3}$.

2.4 CSRCFs from Gaspari and Cohn

In the framework of meteorlogical data assimilation, Gaspari and Cohn (1999) constructed some CSRCFs to approximate the first three autoregressive functions, covariance functions also known as the Gaussian (36), second-order (37) and third-order (38) Markov models (Jordan 1972), respectively:

$$\varphi^{\mathrm{Gauss}}(r,D)=\exp\left(-\frac{r^2}{2D^2}\right), \tag{36}$$

$$\varphi^{\mathrm{Mark2}}(r,D)=\mathrm{e}^{-\frac{r}{D}}\left(1+\frac{r}{D}\right), \tag{37}$$

$$\varphi^{\mathrm{Mark3}}(r,D)=\mathrm{e}^{-\frac{r}{D}}\left(1+\frac{r}{D}+\frac{r^2}{3D^2}\right). \tag{38}$$

By self-convolution of compactly supported functions $B_i(r,a,c)$ $(i=1,2,3)$ of length-scale a and support $[0;c]$,

Gaspari and Cohn obtained three families of CSRBFs φ_i^{GC}:

$$\varphi_i^{\mathrm{GC}}(r,a,c) = (B_i * B_i)\,, \quad (r,a,c). \qquad i = 1,2,3, \tag{39}$$

with support $[0; 2c]$. Specially, for

$$B_1(r,a,c) = \begin{cases} 2(a-1)\frac{r}{c} + 1 & \text{for } 0 \le r \le c/2, \\ 2a(1-\frac{r}{c}) & \text{for } c/2 \le r \le c, \\ 0 & \text{for } r \ge c, \end{cases} \tag{40}$$

Eq. (39) yields the fifth-order polynomial piecewise rational function

$$\varphi_1^{\mathrm{GC}}(r,a,c) = \begin{cases} p_1(r,a) & \text{for } 0 \le r \le c/2, \\ p_2(r,a) + d_2(a)\left(\frac{c}{r}\right) & \text{for } c/2 \le r \le c, \\ p_3(r,a) + d_3(a)\left(\frac{c}{r}\right) & \text{for } c \le r \le 3/2c, \\ p_4(r,a) + d_4(a)\left(\frac{c}{r}\right) & \text{for } 3/2c \le r \le 2c, \\ 0 & \text{for } r \ge 2c, \end{cases} \tag{41}$$

with

$$p_i(r,a) = \sum_{l=0}^{5} b_{i,l}(a)\left(\frac{r}{c}\right)^l \quad (1 \le i \le 4), \tag{42}$$

and where

$$\begin{aligned}
b_{1,5}(a) &= -16\left(3 - 8a + 7a^2\right)/3, \\
b_{1,4}(a) &= +16\left(1 - 2a + 2a^2\right), \\
b_{1,3}(a) &= +10\left(1 - 4a + 8a^2\right), \\
b_{1,2}(a) &= -40\left(1 - 2a + 8a^2\right), /3 \\
b_{1,1}(a) &= 0, \\
b_{1,0}(a) &= 2 + 6a + 44a^2, \\
b_{2,5}(a) &= +16\left(3 - 6a + 5a^2\right)/3, \\
b_{2,4}(a) &= -8\left(2 - 10a + 8a^2\right), \\
b_{2,3}(a) &= +10, \\
b_{2,2}(a) &= +20\left(2 - 22a + 20a^2\right)/3, \\
b_{2,1}(a) &= -5\left(4 - 26a + 36a^2\right), \\
b_{2,0}(a) &= 8 - 35a + 102a^2, \\
b_{3,5}(a) &= +16a\,(2 - 3a)/3, \\
b_{3,4}(a) &= -16a\,(3 - 4a)\,, \\
b_{3,3}(a) &= +40a\,(1 - a)\,, \\
b_{3,2}(a) &= +40a\,(9 - 10a)/3, \\
b_{3,1}(a) &= -10a\,(27 - 22a)\,, \\
b_{3,0}(a) &= a(189 - 122a), \\
b_{4,5}(a) &= +16a^2/3, \\
b_{4,4}(a) &= -32a^2,
\end{aligned} \tag{43}$$

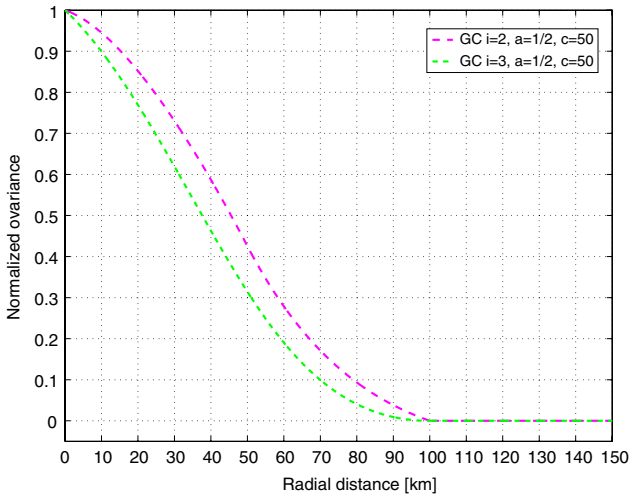

Fig. 4 Examples of Gaspari and Cohn's CSRCFs

$$\begin{aligned}
b_{4,3}(a) &= +40a^2, \\
b_{4,2}(a) &= +320a^2/3, \\
b_{4,1}(a) &= -320a^2, \\
b_{4,0}(a) &= +256a^2, \\
d_2(a) &= \left(-4 + 29a - 42a^2\right)/6, \\
d_3(a) &= -a(243 - 230a)/6, \\
d_4(a) &= -128a^2/3.
\end{aligned}$$

Observe that from the definition of B_0, the length-scale parameter a can get negative values. Furthermore, for some negative values of a, notice that $\varphi_1^{\mathrm{GC}}(r,a,c)$ can be negative (cf. Fig. 4). For $a = 0$ or $a = 1/2$, note that B_0 is a triangular function so expression of $\varphi_1^{\mathrm{GC}}(r,a,c)$ simplifies considerably. As stated in Gaspari et al. (2006), these functions have two continuous derivatives at the origin and approximate the first-order autoregressive function. Moreover, it is straightforward to show that

$$\frac{\partial \varphi_1^{\mathrm{GC}}}{\partial r}(0,a,c) = 0 \quad \forall a, \forall c. \tag{44}$$

To approximate the second-order Markov model (Eq. 37), Gaspari and Cohn proceeded to the convolution of

$$B_2(r,a,c) = \begin{cases} \sqrt{a\left(1 - \mathrm{e}^{-\frac{2c}{a}}\right)}^{-1} \mathrm{e}^{-\frac{r}{a}} & \text{for } 0 \le r \le c, \\ 0 & \text{for } r \ge c, \end{cases} \tag{45}$$

to get

$$\varphi_2^{\mathrm{GC}}(r,a,c) = \alpha \begin{cases} \left(\varphi^{\mathrm{Mark2}}(r,a) - \mathrm{e}^{\frac{r-2c}{a}}\right) & \text{for } 0 \le r \le c, \\ \frac{1}{a}(2c - r)\mathrm{e}^{\frac{-r}{a}} & \text{for } c \le r \le 2c, \\ 0 & \text{for } r \ge 2c \end{cases} \tag{46}$$

with $\alpha = 1/\left(1 - \mathrm{e}^{\frac{-2c}{a}}\right)$. The functions $\varphi_2^{\mathrm{GC}}(r, a, c)$ are non-differentiable at the origin, are always non-negative and tend to the second-order Markov function as c tends to infinity. Figure 3 shows $\varphi_2^{\mathrm{GC}}(r, a, c)$ for arbitrary values of $a = 1/2$ and $c = 50$ km. Finally, setting

$$B_3(r, a, c) = \begin{cases} \mathrm{e}^{-\frac{r}{a}} & \text{for } 0 \le r \le c \\ 0 & \text{for } r \ge c \end{cases} \tag{47}$$

in Eq. (39) and performing the integration leads to the family

$$\varphi_3^{\mathrm{GC}}(r, a, c) = \frac{1}{f_0(a, c)} \begin{cases} f_0(a, c) & \text{for } r = 0, \\ f_1(r, a, c) & \text{for } 0 < r \le c, \\ f_2(r, a, c) & \text{for } c \le r \le 2c, \\ 0 & \text{for } r \ge 2c \end{cases} \tag{48}$$

with

$$f_0(a, c) = a^2 - \left[a^2 + 2c(c + a)\right] \mathrm{e}^{-\frac{2c}{a}} \tag{49}$$

$$f_1(r, a, c) = \frac{r^2 + 3ar + 3a^2}{3} \mathrm{e}^{-\frac{r}{a}} + \frac{2a(c + a)^2}{r} \mathrm{e}^{-\frac{2c}{a}} - \left[\frac{2a(c + a)^2}{r} - 2ac - a^2\right] \mathrm{e}^{\frac{r-2c}{a}} \tag{50}$$

$$f_2(r, a, c) = \frac{2}{r}\left[\frac{r(r + a)(2c - r)}{2} + \frac{(r - c)^3 - c^3}{3} - a(c + a)(r - c + a) + a(c + a)^2 \mathrm{e}^{\frac{r-2c}{a}}\right] \mathrm{e}^{-\frac{r}{a}}. \tag{51}$$

The third-order autoregressive model (Eq. (38)) is obtained by taking the limit of $\varphi_3^{\mathrm{GC}}(r, a, c)$ as c tends to infinity. While φ^{Mark3} is four times continuously differentiable, the compactly supported functionφ_3^{GC} is not even once differentiable at $r = 0$. Moreover, note that any element of this class of CSRCFs is always non-negative; Fig. 3 provides illustrations of examples of such finite covariance functions for arbitrary values of parameters a and c.

3 Computational experiments

This section performs several simulations to study the performance of the CSRCFs presented in Sect. 2.

3.1 Comparisons with the Gaussian, second- and third-order Markov models

These numerical tests begin by analysing the performances of the CSRCFs of Sect. 2 to approximate three of the most popular planar covariance models: the Gaussian (Eq. (36)), the second-order Markov (Eq. (37)) and the third-order Markov (Eq. (38)) models.

To determine the finite covariance functions parameters $(a,\ c)$, three strategies have been investigated:

1. The first method consists in finding the model parameters which minimize the sum of the absolute value of the missfits (difference between the full and finite covariance models) up to the correlation length, i.e.

$$\min \sum_{1 \le i \le \lfloor L^{\mathrm{full}} \rfloor + 1} |\varphi^{\mathrm{full}}(i) - \varphi^{\mathrm{finite}}(i)|, \tag{52}$$

   where subscripts $full$ and $finite$ stand for full and finite covariance models, respectively.
2. With the second strategy, I seek local covariance functions with correlation length equal to the correlation length of the full covariance model.
3. The third method look for the CSRCF with same curvature parameter ξ as the global covariance model to be approximated.

Whereas the first two strategies have an unique solution for each CSRCF model, the third method can give either more than one solution set or no CSRCF with the same curvature parameter as the full covariance model. Therefore, this last method has been forsaken.

Moreover, since Gaspari and Cohn's finite covariance functions of Eqs. (46) and (48) tend to the second-order and third-order Markov models, respectively, as $c \to \infty$, these strategies for the estimation of the CSRCFs parameters led to finite functions with longest supports. Therefore, for comparison purposes, three values for the supports of Gaspari and Cohn's CSRCFS of Eqs. (46) and (48) are used. The first two values have been chosen to be representatives of all the supports estimated for the Wendland's, Wu's and Buhmann's functions. The last value, which is the largest, corresponds to Gaspari and Cohn's functions with correlation length equal to the full covariance function's correlation-length with a drop tolerance of 0.01 km.

Figure 5 (resp. 6 and 7) illustrates that the Gaussian (resp. second-order and third-order Markov) model can be very closely approximated by the compactly supported functions from Wendland, Wu, Buhmann, and Gaspari and Cohn. In these figures as well as in Table 1 which shows corresponding CSRCFs parameters and approximation errors, for each finite function family, I only present the function giving the best fit of the globally supported model. In Table 1,

$$\Delta_1 = \sum_{0 \le i \le \lfloor L^{\mathrm{full}} \rfloor + 1} |\varphi^{\mathrm{full}}(i) - \varphi^{\mathrm{finite}}(i)|, \tag{53}$$

$$\Delta_2 = \sum_{0 \le r \le \lfloor 5001} |\varphi^{\mathrm{full}}(i) - \varphi^{\mathrm{finite}}(i)|. \tag{54}$$

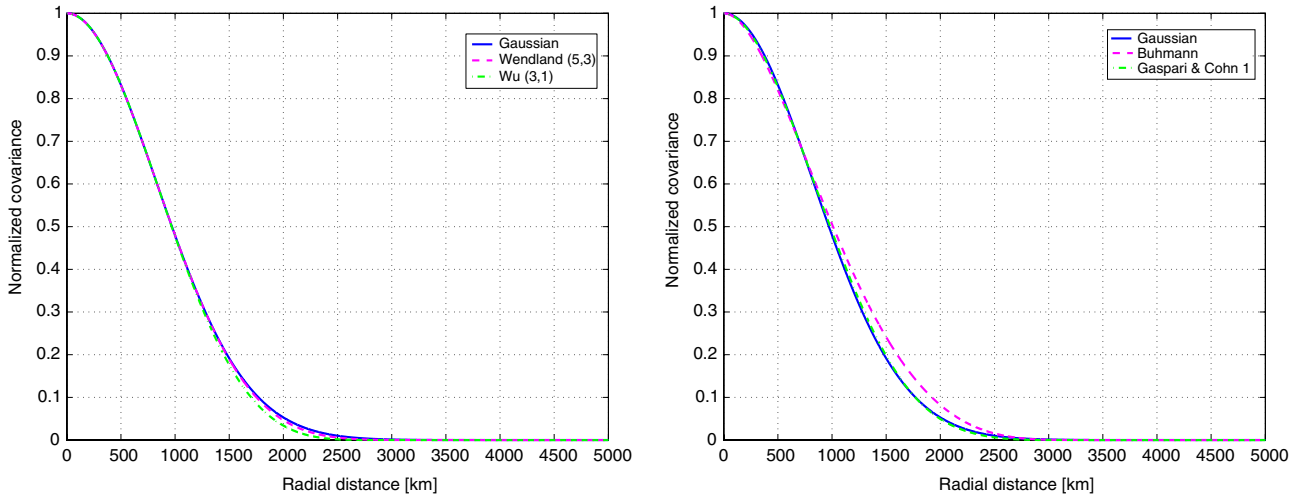

Fig. 5 Comparisons of CSRCFs of Eqs. (13), (27), (33) and (41) with the Gaussian model

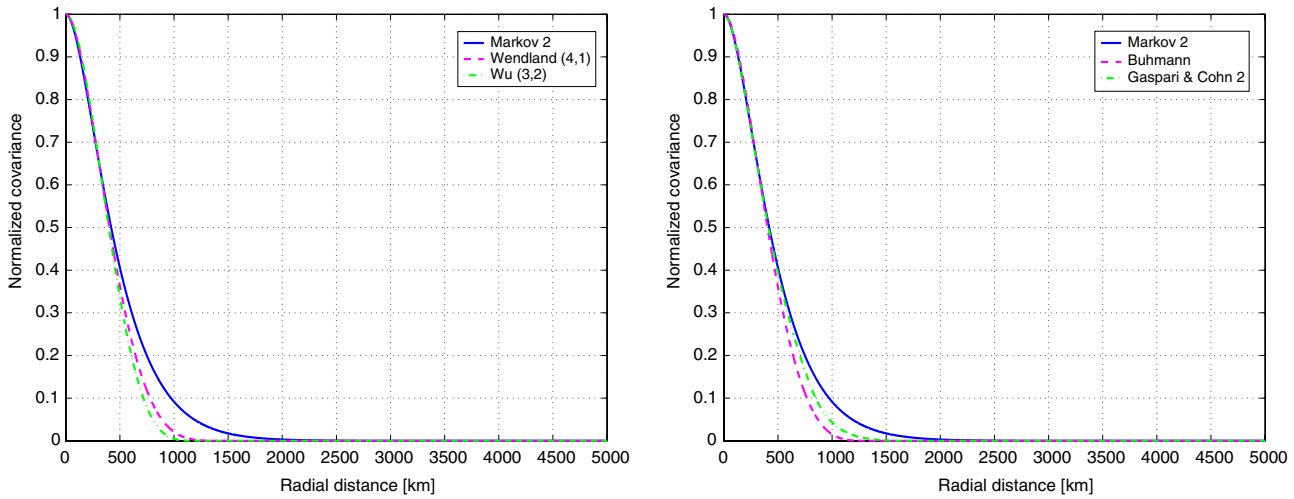

Fig. 6 Comparisons of CSRCFs of Eqs. (10), (28), (33) and (46) with the second-order Markov model

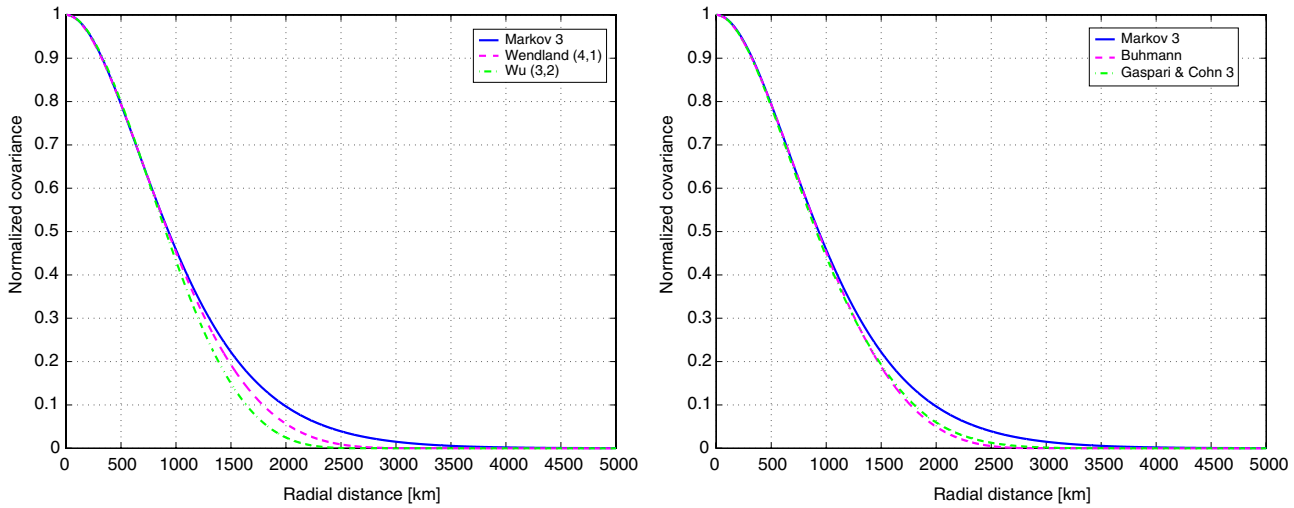

Fig. 7 Comparisons of CSRCFs of Eqs. (10), (28), (33) and (48) with the third-order Markov model

Table 1 Comparison between locally supported approximations of global covariance models

Model	Strategy	c	L_{cor}	Error	
	#	(km)	(km)	Δ_1	Δ_2
Gaussian ($D = 825$ km)	–	–	971.4	–	–
Wendland 53	1	3851	972.3	0.33	7.50
Wendland 53	2	3847	971.4	0.44	8.12
Wu 31	1	3151	968.8	0.26	23.25
Wu 31	2	3159	971.4	0.72	21.90
Buhmann	1	3382	1009.5	8.46	59.99
Buhmann	2	3254	971.4	13.47	36.23
G&C 1 ($a = 0.25$)	1	3196	983.4	3.24	13.24
G&C 1 ($a = 0.25$)	2	3156	971.4	4.80	13.39
Markov 2 ($D = 250$ km)	–	–	419.6	–	–
Wendland 41	1	1526	403.6	3.38	68.17
Wendland 41	2	1587	419.6	5.77	58.11
Wu 32	1	1271	396.7	5.46	89.94
Wu 32	2	1344	419.6	8.88	76.76
Buhmann	1	1351	403.3	3.33	71.72
Buhmann	2	1406	419.6	5.77	61.61
G&C 2	–	1270	398.0	4.76	73.10
G&C 2	–	1590	413.1	1.32	39.93
G&C 2	–	3000	419.6	0.00	2.47
Markov 3 ($D = 400$ km)	–	–	932.1	–	–
Wendland 41	1	3507	927.4	1.09	65.00
Wendland 41	2	3525	932.1	1.64	61.83
Wu 32	1	2905	906.6	3.88	117.07
Wu 32	2	2987	932.1	7.86	102.16
Buhmann	1	3106	927.1	1.24	73.14
Buhmann	2	3123	932.1	1.81	69.78
G&C 3	–	3000	872.6	16.43	130.55
G&C 3	–	3600	910.7	5.36	67.85
G&C 3	–	7000	932.1	0.01	1.66

Note that by definition the first method to estimate the CSRCFs parameters minimizes Δ_1 whereas smallest values of Δ_2 are obtained with the second estimation strategy. Therefore, these first numerical experiences demonstrate that the Gaussian, second-order and third-order Markov models can be accurately approximated by at least one of the CSRCFs of Sect. 2. Note that all of these CSRCFs have simple analytical expressions and provide a large set of quite different functions depending on its parameters. Moreover, observe that the first and second strategy to estimate these parameters give similar results but should be avoided for the second (Eq. (46)) and third (Eq. (48)) Gaspari and Cohn's functions. For these two later finite covariance functions, an alternative to the method used to estimate the third parameters sets could be to compute a and c such that the maximum of the missfit with either the global model or the empirical covariances be equal to a prescribed value.

Table 2 Statistics on de-trended free air gravity anomaliies in the Azores Islands

Number of points	Min (mGal)	Max (mGal)	Mean (mGal)	Std (mGal)
2,601	−55.57	63.66	0.10	11.96
5,776	−56.24	66.39	0.02	13.07
10,201	−56.68	66.39	0.02	13.47

3.2 Interpolation of free air gravity anomalies

The performance of the CSRCFs is assessed using simulated data from the global marine gravity field KMS02 (Andersen et al. 2004). Free-air gravity anomalies have been computed for the area situated near the Azores Islands with the coordinate centre (φ_c, λ_c) at a Northern latitude of 42° and a Western longitude of 30°. The size of the area is 4°-by-4° (see Fig. 8).

From the KMS02 grid of resolution 2′-by-2′, I randomly formed three sets of 2,601, 5,776 and 10,201 observation points, respectively. After removing a fifth order polynomial trend from the data (Fig. 9; Table 2) to get a Gaussian data distribution, an empirical covariance function of the de-trended residuals was computed and modelled by two analytical models: one with an infinite support: Gaussian model (36) for $D = 10$ km, and one with a finite support: Gaspari and Cohn model (41) for $a = 0$ km and $c = 35$ km (see Fig. 10). These covariance model parameters have been estimated by the first strategy of Sect. 3.1, i.e. to give the best fit of the empirical covariances up to its correlation length. All the CSRCFs presented in this paper have been tested to approximate the empirical covariances. The Gaspari and Cohn model (41) has been selcted as it was the model which gave the smallest missfit to both the empirical covariances and the Gaussian model.

Assuming an uncorrelated noise with standard deviation representing 0–1–5% of the signal variance, I predicted free-air gravity anomalies on a regular grid with both the globally (Gaussian) and locally (Gaspari and Cohn) supported covariance functions. The number of prediction points is equal to the number of observations, so is equal to $51^2 = 2{,}601$, $76^2 = 5{,}776$ and $101^2 = 10{,}201$, respectively. Thus, for each subset and each regularization value α, I first computed gravity anomalies vector with the Gaussian covariance model and then compared it with the corresponding vectors from the finite covariance function of Gaspari and Cohn (41). As seen from Fig. 9, free air gravity anomalies interpolated from locally and globally supported covariance models are almost

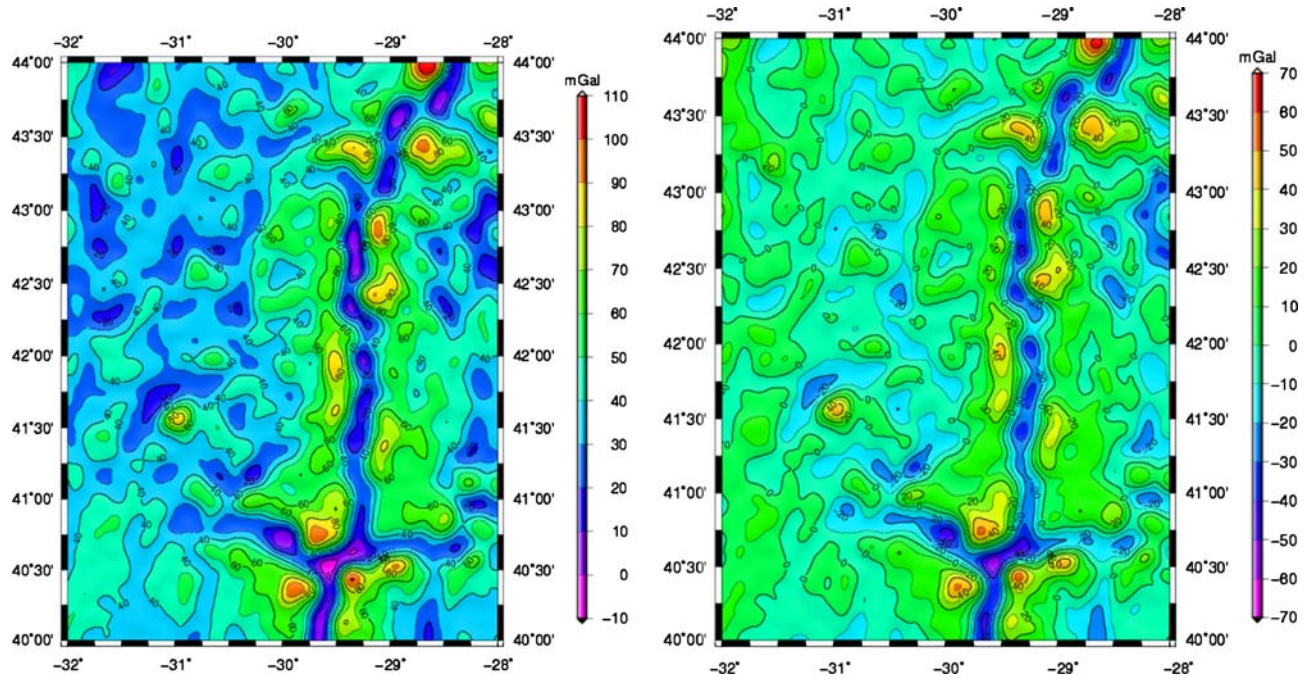

Fig. 8 KMS02 free-air gravity anomaly field from 10,201 observation points (*top*: original; *bottom*: de-trended)

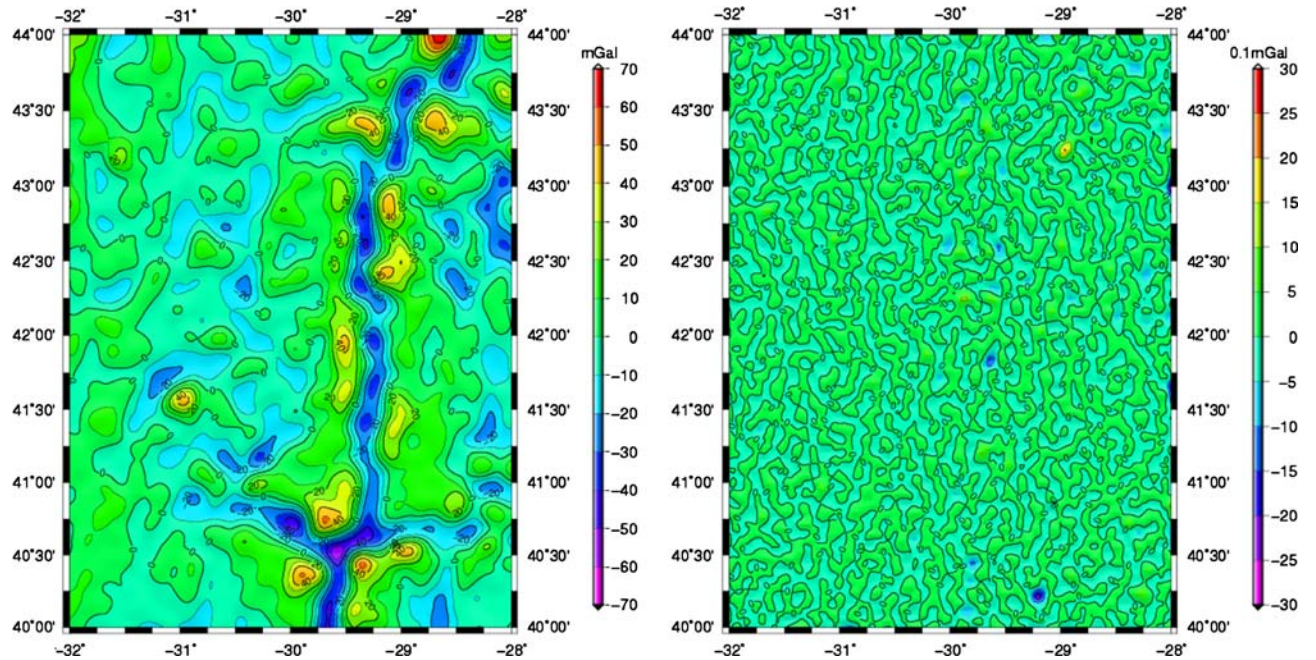

Fig. 9 *Left*: prediction of free-air gravity anomalies with Gaussian model. *Right*: difference between predictions with Gaussian and Gaspari and Cohn (41) models and without regularization

identical and largest differences are observed in area with few observations. Moreover, from Table 3, we notice that the differences between the full and sparse solutions decrease with both increasing observation points number and increasing regularization value. Observe that covariance matrices associated with the finite function require around one fortieth of the full system storage space. Furthermore, histograms (see Fig. 11 as example) indicate that more than 70% (resp. 90%) of the differences between the full and finite predictions are less than 0.25 mGal (resp. 0.5 mGal).

Table 3 Results of free-air gravity anomalies mGal predicted with full (Gaussian) and finite (Gaspari and Cohn) covariance functions

Number of points	Noise (%)		Full (Gaussian)	Finite (G&C 1)	Full - Finite
2,601	0	min	−51.06	−50.64	−3.82
		Max	60.44	62.46	5.30
		Mean	0.04	0.03	0.01
		Std	13.74	13.67	0.79
	1	min	−50.80	−50.75	−2.90
		Max	61.15	62.07	3.87
		Mean	0.04	0.03	0.04
		Std	13.60	13.56	0.53
	5	min	−50.18	−49.88	−1.55
		Max	60.15	61.00	2.71
		Mean	0.04	0.03	0.01
		Std	13.28	13.28	0.26
	Nonzero %		100	2.42	–
5,776	0	min	−54.81	−54.95	−3.26
		Max	65.88	66.43	2.66
		Mean	0.00	0.01	−0.01
		Std	13.82	13.80	0.37
	1	min	−54.66	−55.11	−2.61
		Max	65.58	66.27	2.25
		Mean	0.00	0.01	−0.01
		Std	13.78	13.76	0.35
	5	min	−54.23	−54.99	−1.75
		Max	65.79	66.29	1.60
		Mean	0.01	0.02	−0.01
		Std	13.66	13.64	0.32
	Nonzero %		100	2.39	–
10,201	0	min	−56.26	−56.22	−2.83
		Max	65.87	66.34	2.09
		Mean	0.00	0.01	0.00
		Std	13.82	13.82	0.21
	1	min	−56.00	−56.11	−2.29
		Max	65.61	66.29	2.22
		Mean	0.01	0.01	0.00
		Std	13.80	13.80	0.25
	5	min	−55.62	−55.75	−1.83
		Max	66.00	66.63	1.85
		Mean	0.01	0.02	−0.01
		Std	13.74	13.73	0.29
	Nonzero %		100	2.40	–

As stated in the Introduction, the main advantage of the solution with a finite covariance function is the sparseness of the covariance matrix. A key point is that the Cholseky factor of the sparse matrix will also be sparse. In fact, if the sparse covariance matrix is properly ordered, then its

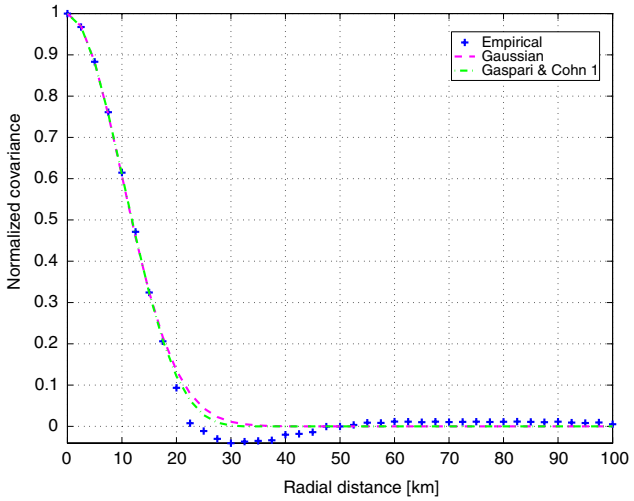

Fig. 10 Normalized covariance functions of free-air gravity anomalies in Azores Islands

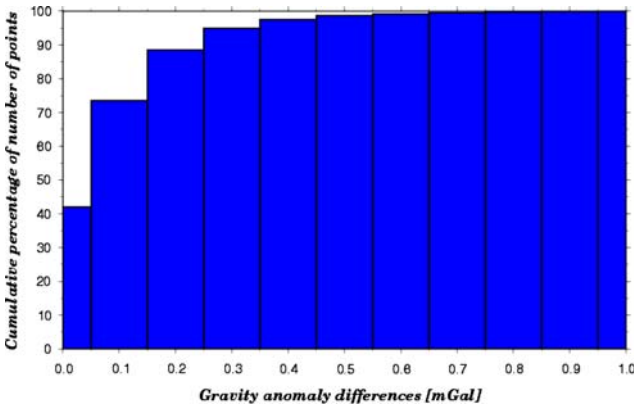

Fig. 11 Differences between 10,201 free-air gravity anomalies predicted with the Gaussian and Gaspari and Cohn model without regularization

Cholesky factor is sparse while the inverse of the sparse covariance matrix is not necessarily sparse. To increase the efficiency in terms of memory and CPU time of using sparse covariance matrices (i.e. locally supported covariance functions), one has to order the covariance matrix so it and its Cholesky factor have the smallest number of nonzero entries. Three commonly used techniques of ordering are natural ordering, the reverse Cuthill–McKee algorithm (Cuthill and McKee 1969) and the minimum degree reordering algorithm (George and Liu 1989). The matrix structures after reordering are plotted in the first column of Fig. 12, while the pattern of the nonzero entries of the corresponding Cholesky factors are depicted by the second column of Fig. 12. These matrices correspond to the matrices associated with the 10,201 KMS02 observation points.

The natural ordering is the simpliest and easiest way to build the covariance matrix. It consists in numbering the observation points from the bottom-left corner to the top-right

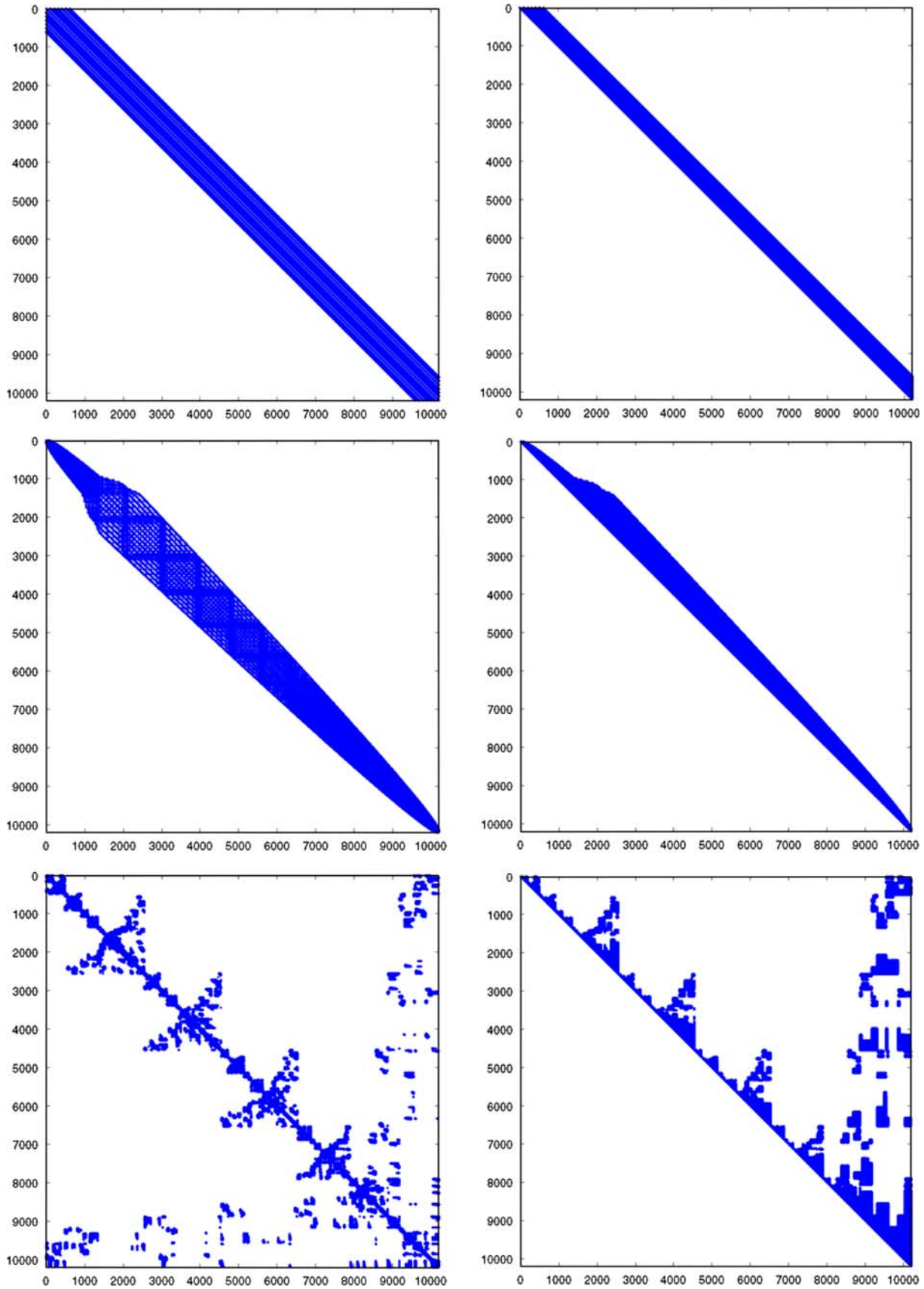

Fig. 12 Influence of ordering on structure of normal matrices (*left*) and corresponding Cholesky factors (*right*). The first row is for a natural numbering, the second row is after a reverse Cuthill-McKee reordering, the last after a minimum-degree reordering

corner, i.e. by ascending latitude and ascending longitude. Therefore, this ordering scheme is particularly adapted to gridded data points. However, it produces a covariance matrix with the biggest bandwidth when compared with two others ordering techniques. Moreover, this band contains a non-negligible number of zeros. The reverse Cuthill–McKee algorithm produces a matrix with a narrow bandwidth and generally makes nonzero elements display along the main diagonal. The minimum degree procedure produces a structure with large blocks of continuous zeros, as shown in the third row of Fig. 12. Note that the Cholesky factor has at least the same nonzeros as the lower triangular part of the covariance matrix, but usually some new nonzero entries arise in the Cholesky factor. This new nonzero elements are fill-in elements. To reduce the amount of fill-in elements, the most popular solution consists to replace the estimation of the exact or complete Cholesky decomposition by the computation of an incomplete factorization of the covariance matrix (George and Liu 1981; Saad 1996). For more details on ordering strategies to reduce fill-in in Cholesky factorization of geodetic covariance matrices, see Jonge de (1992).

4 Conclusions and discussion

In this study, I have demonstrated that compactly supported radial covariance functions from Wendland, Wu, Buhmann and Gaspari and Cohn (see Sect. 2) with simple analytical expressions can accurately approximate three of the most well-known planar covariance models: the Gaussian, second-order and third-order Markov functions (cf. Sect. 3.1). Then, interpolations of KMS02 free-air gravity anomalies by both global (Gaussian) and local (Gaspari and Cohn) covariance functions have shown the capability of CSRCFs to be successfully (in terms of both prediction differences and memory savings) substituted to globally supported covariance models. Furthermore, these numerical experiments (see Sect. 3.2) have also pointed out that differences between predictions with global and local models decrease with increasing the number of observation points as well as with increasing the magnitude of the regularization term.

However, such good results strongly depend on the CSRCFs parameterization as well as on the ordering scheme of the sparse covariance matrix. Moreover, note that this strategy can only be applied if the empirical or global model covariances are negligible with respect to the variance beyond a fixed distance. To be effective, sparse linear solvers should not be used with matrices for which the number of non-zero elements exceeds 3%. For practical purposes, I recommend to estimate the CSRCFs parameters in order to get the locally supported covariance function which has its correlation-length equal to the correlation-length of either the empirical or the global model covariances.

Therefore, the use of CSRCFs makes a variety of applications that were previously impractical with globally supported covariance functions on personal computers. Meanwhile, further testing is required before we can defintely status on the goodness of this method in geodesy. Until know, finite covariance functions have only been tested in the framework of interpolation problems with homogeneous data (i.e. data associated with the same functional of the anomaly gravity field). Thus, in a forthcoming paper, following the approach of Weber and Talkner (1993), I will begin by extending these CSRCFs to the spherical case, compare its performances with the globally supported spherical models from Tscherning and Rapp (1974) as well as with existing finite covariance functions from Sansò and Schuh (1987) and Moreaux (2001), and then address its use with heterogeneous data. Based on the idea from Arabelos and Tscherning (1999), in this next paper, finite covariance functions will also be used to approximate not only the signal but also the error covariance matrix. Finally, this strategy should also be compared with other techniques such as optimal interpolation, sampling methods (Achlioptas et al. 2002) and multizone decomposition (Fieguth et al. 1995) which enable to deal with large datasets on standard computers.

Acknowledgements The author is grateful to the three anonymous reviewers of this paper for extremely valuable comments and suggestions for improvement of the original manuscript. I would also thank to my wife Patricia for her unconditional support as well as my precious librarian: Françoise.

References

Achlioptas D, McSherry F, Schölopf B (2002) Sampling techniques for kernel methods. Adv Neur Inf Proc Syst 14:335–342

Andersen OB, Knudsen P, Trimmer R (2004) Improving high resolution altimetric gravity field mapping (KMS2002 Global marine gravity field). In: Sansò F (ed.) A window on the future of geodesy. Springer, Berlin. IAG Symposia 128:326–331

Arabelos D, Tscherning CC (1996) Collocation with finite covariance functions. Int Geoid Serv Bull 5:117–136

Arabelos D, Tscherning CC (1999) Gravity field recovery from airborne gradiometer data using collocation and taking into account correlated errors. Phys Chem Earth(A) 24(1):19–25

Askey R (1973) Radial characteristic functions. MRC Report 1262, University of Wisconsin, Madison

Buhmann MD (2000) A new class of radial basis functions with compact support. Math Comput 70:307–318. doi: 10.1090/S0025-5718-00-01251-5

Cuthill E, McKee J (1969) Reducing the bandwidth of sparse symmetric matrices. In: Proceedings of the 24th National Conference on ACM, New York, pp 157–172

Fieguth PW, Karl WC, Willsky AS, Wunsch C (1995) Milterosolution optimal interpolation and statistical analysis of TOPEX/POSEIDON satellite altimetry. IEEE Tans Geosci Remote Sens 33(2):280–292

Floater MS, Iske A (1996) Multistep scattered data interpolation using compactly supported radial basis functions. J Comp Appl Math 73:65–78

Fornefett M, Rohr K, Stiehl HS (1999) Elastic registration of medical images using radial basis functions with compact support. In: Proceedings of the Computer Vision and Pattern Recognition, Fort Collins, USA, June 23–25, pp 402–407

Furrer R, Genton MG, Nychka D (2005) Covariance tapering for interpolation of large spatial datasets. J Comput Graph Stat 15(3):502–523. doi: 10.1198/106186006X132178

Gaspari G, Cohn SE (1999) Construction of correlation functions in two and three dimensions. Quart J R Meteorol Soc 125:723–757

Gaspari G, Cohn SE, Guo J, Pawson S (2006) Construction and application of covariance functions with variable length-fields. Quart J R Meteorol Soc 132:1815–1838. doi: 10.1256/qj.05.08

George A, Liu JWH (1981) Computer solution of large sparse positive definite matrices. Prentice Hall, Englewood Cliffs

George A, Liu JWH (1989) The evolution of the minimum degree algorithm. SIAM Rev 31:1–19

Gneiting T (1999) Correlation functions for atmospheric data analysis. Q J R Meteorol Soc 125:2449–2464

Hon YC, Zhou X (2000) A comparison on using various radial basis functions for options pricing. Int J Appl Sci Comput 7:29–47

Jonge de PJ (1992) A comparative study of algorithms for reducing the fill-in during Cholesky factorization. Bull Geod 66:296–305

Jordan SK (1972) Self-consistent statistical models for the gravity anomaly, vertical deflections, and undulation of the geoid. J Geophys Res 77:3660–3670

Kasper JF (1971) A second-order Markov gravity anomaly model. J Geophys Res 76(32):7844–7849

Kusche J (2001) Implementation of multigrid solvers for satellite gravity anomaly recovery. J Geod 74:773–782

Moreaux G, Tscherning CC, F Sansò (1999) Approximation of harmonic covariance functions on the sphere by non-harmonic locally supported ones. J Geod 73:555–567

Moreaux G (2001) Some preconditioners of harmonic spherical spline problems. Inverse Problems 17:157–177

Moritz H (1989) Advanced physical geodesy 2nd edn. Wichmann, Karlsruhe

Morse BS, Yoo TS, Rheingans P, Chen DT, Subramanian KR (2001) Interpolating implicit surfaces from scattered surface data using compactly supported radial basis functions. In: Proceedings of the International conference on shape modeling and applications, Genova, Italy, pp 89–98

Rygaard-Hjalsted C, Constable CG, Parker RL (1997) The influence of correlated crustal signals in modelling the main geomagnetic field. Geophys J Int 130:717–726

Saad Y (1996) Iterative methods for sparse linear system 1st edn. The PWS Series in Computer SCience, PWS Publishing, Boston, http://www-users.cs.umm.edu/~saad/books.html

Sansò F, Schuh WD (1987) Finite covariance functions. Bull Geod 61:331–347

Schaback R, Wendland H (1993) Special cases of compactly supported radial basis functions. Manuscript, Göttingen

Schreiner M (1997) Locally supported kernels for spherical spline interpolation. J Approx Theory 89:172–194

Tscherning CC, Rapp RH (1974) Closed covariance expressions for gravity anomalies, geoid undulations and deflections of the vertical implied by anomaly degree variance models. Department of Geodetic Science, Report 208, The Ohio State University, Columbus

Tóth G, Völgyesi L (2007) Local gravity field modeling using surface gravity gradient measurements. Tregoning P, Rizos C (eds.) Dynamic planet monitoring and understanding a dynamic planet with geodetic and oceanographic tools. Springer, Berlin. IAG Symposia 130:424–429

Wachowiak MP, Wang X, Fenster A, Peters TM (2004) Compact support radial basis functions for soft tissue deformation. In: Proceedings of IEEE International Symposium on Biomedical Imaging, Arlington, Virginia, pp 1259–1262

Weber RO, Talkner P (1993) Some remarks on spatial correlation function models. Mon Weather Rev 121:2611–2617

Wendland H (1995) Piecewise polynomial, positive definite and compactly supported radial basis functions of minimal degree. Adv Comput Math 4:389–396

Wendland H (1998) Error estimates for interpolation by compactly supported radial basis functions of minimal degree. J Approx Theory 93:258–272

Wendland H (2002) Compactly supported correlation functions. J Multivariate Anal 83:493–508. doi: 10.1006/jmva.2001.2056

Wong SM, Hon YC, Li TS (1999) Radial basis functions with compact support and multizone decomposition: applications to environmental modelling. Bound Elem Technol 13:355–364

Wu Z (1995) Compactly supported positive definite radial functions. Adv Comput Math 4:283–292